

Effects of uniaxial stress and temperature variation on the Cr^{2+} center in GaAs

J. J. Krebs and G. H. Stauss

Naval Research Laboratory, Washington, D. C. 20375

(Received 5 February 1979)

The effects both of applied uniaxial stress and of temperature variation on the EPR spectrum of Cr^{2+} in GaAs have been studied. The rapid stress-induced alignment of the Cr^{2+} centers at 4.2 K shows that the observed tetragonal symmetry is due to the Jahn-Teller effect as was previously suggested. The Jahn-Teller coefficient V_E for an E -symmetry distortion mode is 0.85 ± 0.09 eV/Å and the Jahn-Teller splitting $3E_{JT}$ of the ground 5T_2 manifold is estimated. Stress has only a small effect on the spin-Hamiltonian parameters in agreement with the large E_{JT} found. When taken together with previous optical work the results imply a significant Jahn-Teller splitting in the 5E state also. The EPR lines broaden in the 9–20-K temperature range and the temperature-dependent linewidth parameter T_2^{-1} is deduced from both the observed signal amplitudes and linewidths of the inhomogeneously broadened lines. The relation $T_2^{-1} = (T_2^{-1})_0 \exp(-\Delta E/kT)$ is obeyed with $\Delta E = 67 \pm 5$ cm $^{-1}$. Comparison with recent ultrasonic attenuation studies in GaAs:Cr shows that $T_2^{-1} \approx \tau^{-1}$, the Cr^{2+} reorientation rate. The dependence of T_2^{-1} on temperature is probably due to motional broadening.

I. INTRODUCTION

In this paper we report the effects both of applied uniaxial stress and of temperature on the EPR spectrum of the Cr^{2+} center in GaAs. The stress results confirm that the low-symmetry EPR spectrum found earlier¹ arises from a static Jahn-Teller effect and also allow us to estimate the Jahn-Teller energy. Line broadening is observed in the 10–20-K range and is shown to be due to thermally induced reorientation of the Cr^{2+} distortion axis by comparison with recent ultrasonic attenuation work.²

The singly filled acceptor state of Cr in GaAs is $\text{Cr}^{2+}(3d^4)$. Its ground-state energy and that of the neutral acceptor Cr^{3+} lie deep within the forbidden energy gap of GaAs. This gives rise to the semi-insulating properties of Cr-doped GaAs which have proven so useful for GaAs device substrate use. While chromium is apparently substitutional for Ga in GaAs, the EPR spectrum of Cr^{2+} shows that the center has tetragonal (D_{2d}) symmetry rather than the full cubic (T_d) symmetry of a normal Ga site.

We have attributed¹ this lowered symmetry to a Jahn-Teller effect which is static for temperatures below 10 K. One basis for this interpretation was the observation that one can change the charge state of Cr by illuminating the sample with infrared light. Each of the charge states (3+, 2+, 1+) has a different site symmetry and the ability to interconvert significant population fractions between these states argues strongly for a Jahn-Teller rather than for an associated defect explanation of the lowered symmetry. A second basis was the close similarity between the behavior of Cr^{2+} in GaAs and in the

II–VI compounds which have the same zinc-blende structure. Vallin and Watkins (VW)³ concluded that in each of the cubic crystals ZnS, ZnSe, ZnTe, and CdTe, and in hexagonal ZnS and CdS, one finds Cr^{2+} in a Jahn-Teller distorted ground state with D_{2d} symmetry. Their definitive test of the Jahn-Teller explanation in the II–VI's was the ease with which applied uniaxial stress can cause reorientation of the Cr^{2+} -center distortion axis at low temperatures.

In spite of the above arguments which support a Jahn-Teller interpretation for the GaAs:Cr²⁺ site symmetry, it was thought that this explanation should be verified by carrying out low-temperature applied-stress experiments, especially since in GaAs Cr^{2+} might require some sort of local charge compensation not needed for the II–VI compounds. These experiments have also allowed us to determine how uniform strain affects the relative energies of the differently oriented centers. Quantitative measurements of the temperature-dependent line broadening were also carried out and proved quite useful.

At low temperatures there are equal numbers of Cr^{2+} centers distorted along each of the $\langle 100 \rangle$ directions. This distortion produces an orbital singlet ground state ${}^5\hat{B}_2$ having a spin $S = 2$ and a spin Hamiltonian

$$\begin{aligned} \mathcal{H} = & g_{\parallel}\mu_B S_z H_z + g_{\perp}\mu_B (S_x H_x + S_y H_y) \\ & + DS_z^2 + \left(\frac{1}{6}a\right)(S_x^4 + S_y^4 + S_z^4) \\ & + \left(\frac{1}{180}F\right)(35S_z^4 - 15S_z^2) \quad , \end{aligned} \quad (1)$$

for which the parameters have been determined earlier.¹ If the distortion is Jahn-Teller induced, the en-

ergy of the ground state is particularly sensitive to strain and for D_{2d} symmetry has the form³

$$E_s^i = V_{ES}e_\theta^i + V_{AS}e_1 \quad (2)$$

where E_s^i is the strain dependent energy for the i th type of distortion, $e_\theta^i \equiv e_{zz}^i - \frac{1}{2}(e_{xx}^i + e_{yy}^i)$ is the E_θ type strain referred to the local z axis, $e_1 \equiv e_{xx} + e_{yy} + e_{zz}$ is the isotropic volume strain, and V_{ES} (V_{AS}) is the coefficient for strain belonging to the E (A_1) representation of T_d . Note that the term $V_{AS}e_1$ is the same for all Cr^{2+} centers for a uniform strain.

For a general applied stress the E_s^i are different and the populations p_i of the variously distorted centers will follow a Boltzmann distribution with

$$p_i/p_j = \exp[-(E_s^i - E_s^j)/kT] \quad .$$

Thus by measuring the population changes produced by applied stress one can determine V_{ES} (but not V_{AS}). For definiteness, we let a , b , and c be those Cr^{2+} centers distorted along [100], [010], and [001], respectively. For [001] stress P one then has

$$e_\theta^a = -2e_\theta^{b,c} = -(s_{11} - s_{12})P \quad ,$$

for [111] stress the e_θ^i all vanish, and for [011] stress

$$e_\theta^a = -2e_\theta^{b,c} = \frac{1}{2}(s_{11} - s_{12})P \quad .$$

Here s_{11} and s_{12} are the elastic moduli of GaAs which are assumed to be unaltered locally by the presence of Cr.

II. EXPERIMENTAL METHOD

Samples of Cr-doped GaAs were obtained from various sources, x-ray aligned, and cut to the desired dimensions (typically $1 \times 4 \times 12 \text{ mm}^3$). The long (stress) axis was along the [001], [111], or [011] crystallographic direction for different samples. Care was taken to grind the sample ends accurately perpendicular to the stress axis. Uniaxial compressive stress was applied to the sample while it was bathed in liquid helium using a stress rod and lever system similar to that of Watkins and Corbett.⁴ The Teflon piston and anvil were made in the form of nesting cups to assure proper alignment. Friction was found to be negligible. Because of thermal depopulation of the resonant spin states and consequent weak signals at lower temperatures, stress data were taken only at 4.2 K.

The EPR signals from the Cr^{2+} centers were measured with a modified Varian E-9 X-band spectrometer. A TE_{011} microwave cavity was constructed of low-temperature Hysol using the silvering techniques suggested by Van Camp and co-workers⁵ in order to allow 100-kHz field modulation in the liquid-helium temperature range. Because of the large line widths ($\geq 90 \text{ G}$) and low Cr^{2+} concentrations [$(2-5) \times 10^{16}$

cm^{-3}], almost all data were taken with the magnetic field along high-symmetry directions to maximize the signal-to-noise ratio. The temperature-dependent linewidth data were taken using the EPR apparatus described earlier.⁶

III. RESULTS AND DISCUSSION

A. Stress effects

By applying stress along the [001] direction it is possible to align all the Cr^{2+} centers along the stress direction. This alignment occurs in less than 1 sec at 4.2 K showing that the distortion is indeed Jahn-Teller generated and consists of a local compression along a (100) direction. Typical data are shown in Fig. 1 where the integrated intensity of the EPR line for a type- c Cr^{2+} center is plotted as a function of the applied stress. As can be seen, the intensity of this line increases with stress and saturates at three times the initial value. This is the increase expected upon alignment if the a -, b -, and c -type centers were equally populated initially. The low-stress data can be analyzed to determine the value of V_{ES} .

For stress along the [011] direction the derived value of V_{ES} is roughly 20% larger than for [001] stress. However, this data is not reliable since there is some apparent loss in the total integrated Cr^{2+} EPR intensity when [011] stress is applied. Stress along the [111] direction has no effect on the EPR line intensities. This shows that T_2 -type modes do not couple strongly to the Cr^{2+} center, as is consistent with the D_{2d} symmetry observed.

The behavior of the EPR intensity I from c -type

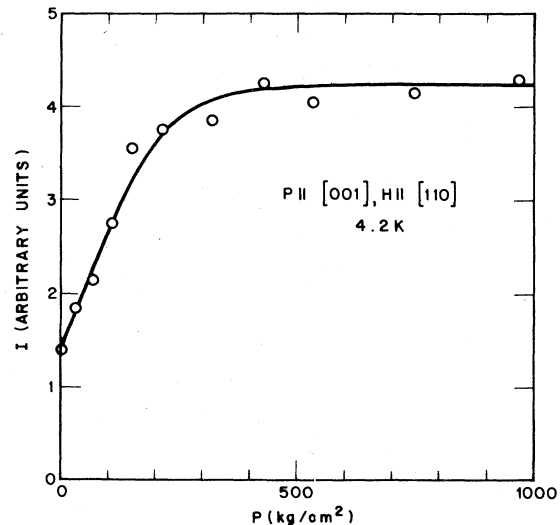


FIG. 1. Stress alignment of the Cr^{2+} c -type centers for stress along the distortion axis.

centers follows from Eq. (2). For [001] stress P

$$I/I_s = [1 + 2 \exp(-3\alpha P/kT)]^{-1} \quad (3)$$

where I_s is the intensity at saturation and $\alpha = \frac{1}{2} V_{ES}(s_{11} - s_{12})$. One finds $\alpha = 2.3 \times 10^{-24} \text{ cm}^3$ from the slope of $\log(I_s/I - 1)$ vs P as shown in Fig. 2. The solid curve in Fig. 1 was obtained using Eq. (3) and this value of α .

The Jahn-Teller coupling which drives the tetragonal distortion of a T_2 state is given⁷ by $V_E \times (Q_\theta \mathcal{E}_\theta + Q_e \mathcal{E}_e)$ where Q_θ, Q_e are E -type distortion modes of the complex and $\mathcal{E}_\theta, \mathcal{E}_e$ are electronic operators spanning T_2 . Assuming a local cluster model for a zinc-blende structure one can show⁸ that V_{ES} and V_E are related by

$$V_{ES} = \frac{2}{3} \sqrt{2} R V_E, \quad (4)$$

where R is the nearest-neighbor distance (2.443 Å for GaAs). The room-temperature elastic moduli of GaAs have been measured⁹ to be $s_{11} = 1.16 \times 10^{-12} \text{ cm}^2/\text{dyne}$ and $s_{12} = -0.31 \times 10^{-2} \text{ cm}^2/\text{dyne}$. Using Eq. (4) one finds the Jahn-Teller coupling coefficient V_E to be $0.85 \pm 0.09 \text{ eV}/\text{Å}$. In Table I this value is compared with the Cr^{2+} V_E values found for the II-VI zinc-blende lattices.³ The GaAs value is seen to be two to three times that of the II-VI's.

One may now estimate the Jahn-Teller energy E_{JT} using the expression⁷

$$E_{JT} = V_E^2 / 2M\omega_E, \quad (5)$$

where M is a ligand mass and ω_E is the frequency of the local mode which couples to the Cr^{2+} ion. The value of E_{JT} found in this manner is shown in Table I. The value of $\hbar\omega_E$ was taken to be 78 cm^{-1} based on the luminescence results¹⁰ for Cr^{2+} in GaAs which show that this is the lowest energy mode excited by the ${}^5E \rightarrow {}^5T_2$ transition. We take this to be an E

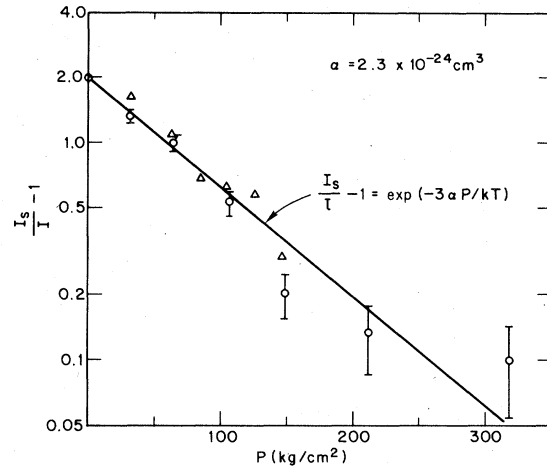


FIG. 2. Evaluation of α from the low-stress data for c -type Cr^{2+} centers for $P \parallel [001]$ and 4.2 K. Different symbols represent data from different runs.

mode. It should be noted, however, that neutron-diffraction results¹¹ indicate that the pure GaAs phonon mode at 79 cm^{-1} is $\text{TA}(X)$ while the $\text{TA}(L)$ mode which can produce¹² an E -type mode occurs at 62 cm^{-1} . The Cr^{2+} E_{JT} values for the II-VI compounds are also shown in Table I.

The Jahn-Teller distortion splits the 5T_2 state as shown in Fig. 3 by an amount $3E_{JT}$. For GaAs: Cr^{2+} this results in a rather large splitting of $5200 \pm 1100 \text{ cm}^{-1}$. In principle the 5E state can also be split as shown. The ratio of the 5E and 5T_2 splittings is given¹² by $\rho = V_E({}^5E)/V_E({}^5T_2)$ for a given distortion Q_θ . Both luminescence^{10,13} and optical-absorption¹³ data locate the Cr^{2+} 5E - 5T_2 zero-phonon line at 6760 cm^{-1} , while the peak¹⁴ of this optical absorption is at 7300 cm^{-1} . If we use the model calculations of Valin *et al.*¹² for Cr^{2+} , the available data can be fit with the following parameters: the cubic crystal field splitting $\Delta = 5500 \text{ cm}^{-1}$, $E({}^5\hat{E}) - E({}^5\hat{B}_2) = 3E_{JT} = 4500 \text{ cm}^{-1}$, and $\rho = -0.40$ so that ${}^5\hat{A}_1$ lies below ${}^5\hat{B}_1$ and both absorption and luminescence occur between ${}^5\hat{B}_2$

TABLE I. Cr^{2+} Jahn-Teller parameters for GaAs and the II-VI zinc-blende compounds.

Compound	$-V_E$ (eV/Å)	$\hbar\omega_E$ (cm^{-1})	E_{JT} (cm^{-1})	Reference
GaAs	0.85 ± 0.09	78	$\sim 1720^a$	This work
ZnSe	> 0.40	69	> 470	Ref. 3
ZnTe	≥ 0.32	67	≥ 200	Ref. 3
CdTe	≥ 0.34	42	≥ 560	Ref. 3

^aEstimated error $\pm 350 \text{ cm}^{-1}$.

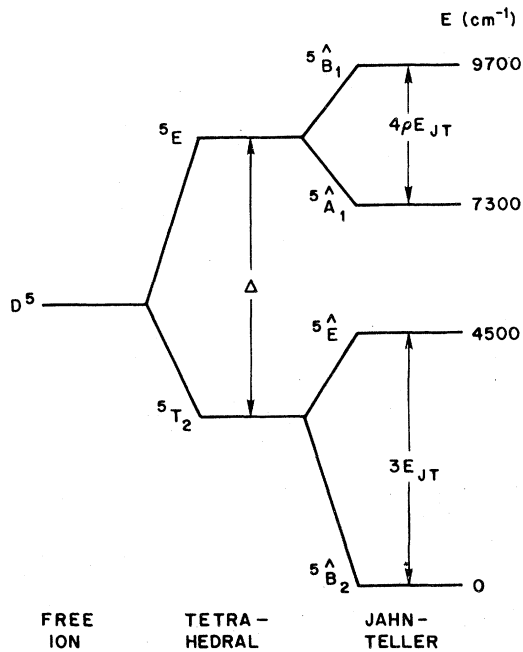


FIG. 3. Splitting of the ${}^5D(3d^4)$ manifold under the combined action of the tetrahedral crystal field and the Jahn-Teller distortion. Parameters used are $\Delta = 5500 \text{ cm}^{-1}$, $E_{JT} = 1500 \text{ cm}^{-1}$, and $\rho = -0.40$. The energies are evaluated at the equilibrium ground-state distortion.

and 5A_1 . The above parameters stem from a choice of E_{JT} near the lower limit of the experimentally determined range and are meant to be illustrative rather than definitive. Nevertheless, the above data do require a negative ρ significantly different from zero. (For the Cr^{2+} in the II-VI compounds¹² $\rho \approx 0$.) The cubic field splitting seems reasonable compared to that in the II-VI's ($\Delta \approx 4500 \text{ cm}^{-1}$). One reason for choosing the low value of E_{JT} is that Eq. (5) probably overestimates E_{JT} since anharmonicity is neglected. (Note that even for $E_{JT} = 1500 \text{ cm}^{-1}$, $\bar{Q}_\theta = 0.44 \text{ \AA}$ which is almost 20% of the nearest-neighbor distance. The unverifiable assumptions needed to evaluate V_E above also decrease the accuracy of E_{JT} .)

Vallin and Watkins³ have pointed out that the Cr^{2+} spin Hamiltonian Eq. (1) must be augmented by

strain dependent terms. For D_{2d} symmetry these have the form

$$\mathcal{H}_e = c_1 e_1 S_\theta + c_2 e_\theta S_\theta + c_3 e_e S_e + c_4 e_\zeta S_\zeta + c_5 (e_\xi S_\xi + e_\eta S_\eta) \quad (6)$$

where the c_i are new spin-Hamiltonian parameters and the expressions for the strains e_i and second-order spin operators S_i can be found in Ref. 3. We find that only for $\bar{\Gamma}||[111]$ is a line shift observed which is a measurable fraction of the linewidth. If, as the experimental and theoretical results of VW suggest, one can neglect c_1 , then the available data permit one to determine c_4 and set an upper limit on c_2 . Table II lists these values and compares them with the CdTe results.³ The Cr^{2+} spin Hamiltonian is seen to be much less sensitive to strain in GaAs than in CdTe. This is consistent with the larger value of E_{JT} since to a first approximation c_2 and c_4 are proportional³ to $(E_{JT})^{-2}$.

When the samples are stressed, some of the Cr^{2+} EPR lines broaden as VW found for the II-VI compounds. Unlike VW, however, we cannot attribute this to inhomogeneous strain since the strain-dependent line shifts observed are too small for such an explanation. The origin of this stress broadening in GaAs remains unclear.

B. Temperature effects

The temperature-dependent broadening of the Cr^{2+} EPR lines in GaAs was measured in the range of 4–20 K. Below 9 K the linewidths are constant ($\sim 90 \text{ G}$ between derivative extrema) and presumably governed by superhyperfine interactions with the surrounding As and Ga nuclei. With increasing temperature the lines broaden and finally disappear for $T > 20 \text{ K}$. Simultaneously the Gaussian line shape becomes nearly Lorentzian. In order to unfold the temperature-dependent broadening from the linewidth data, we assume that the low-temperature Gaussian line is made up of a larger number of narrow Lorentzian components. A computer simulation shows that when the Lorentzian to Gaussian linewidth ratio W_L/W_G is allowed to increase the observed linewidth will increase and the derivative am-

TABLE II. Strain-coupling spin-Hamiltonian coefficients for Cr^{2+} in GaAs and CdTe. All are in units of cm^{-1}

Compound	c_1	c_2	c_3	c_4	c_5	Reference
GaAs	0 ^a	$\leq +9$	b	+7.2	b	This work
CdTe	-2	+40	-10	+40	+30	Ref. 3

^aAssumed zero in line with the results of Ref. 3.

^bNot determined.

plitude will drop rapidly. The results of this simulation are given in the Appendix since they may prove useful for other EPR systems.

By using either (i) the observed linewidth or (ii) that part of the decrease in signal amplitude which is in excess of the Boltzmann population effect, one can find W_L/W_G as a function of temperature. The results of such an analysis are shown in Fig. 4 for the $S_z = 0 \rightarrow S_z = +1$ EPR line with $\vec{H} \parallel [001]$. Similar results are found for the $-1 \rightarrow +1$ line. To make contact with the related work of VW we note that the linewidth parameter

$$T_2^{-1} = \frac{1}{2} \sqrt{3} \gamma W_L = 1.37 \times 10^9 \times (W_L/W_G),$$

where the γ is the gyromagnetic ratio and $W_G = 90$ G. From Fig. 4 it appears that T_2^{-1} obeys an Arrhenius law,

$$T_2^{-1} = (T_2^{-1})_0 \exp(-\Delta E/kT). \quad (7)$$

Based on all the available data the best parameters for GaAs:Cr²⁺ are $\Delta E = 67 \pm 5$ cm⁻¹ (0.0083 eV) and

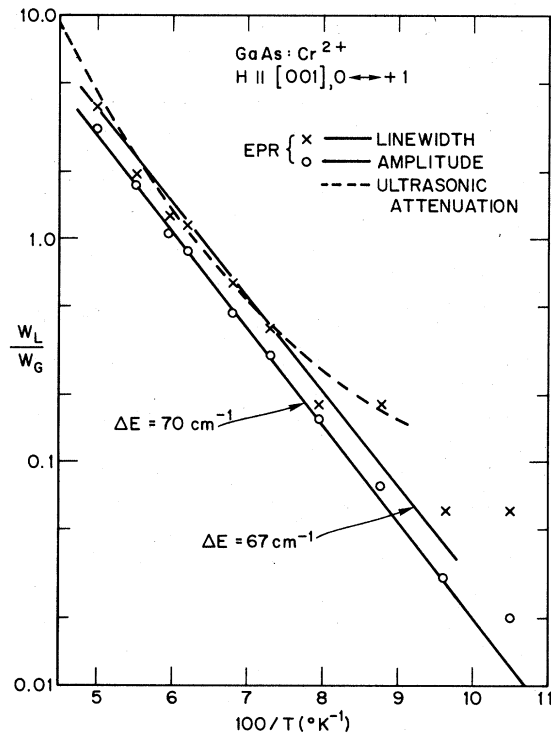


FIG. 4. Lorentzian-to-Gaussian linewidth ratios (W_L/W_G) derived from analysis of the temperature-dependent EPR derivative linewidth and amplitude. The straight lines represent the expression $W_L = W_G^0 \exp(-\Delta E/kT)$. The dashed curve represents the reorientation rates τ^{-1} determined by ultrasonic attenuation (see text).

$(T_2^{-1})_0 \approx 4.9 \times 10^{11}$ sec⁻¹. These values fall in the range which VW found for the II-VI compounds.

Very recently Tokumoto and Ishiguro have studied² the frequency and temperature dependence of ultrasonic attenuation in Cr-doped GaAs. They find that only *E*-type modes are attenuated and they attribute this to losses associated with reorientation of the Cr²⁺ centers found previously by EPR. They express the reorientation rate as

$$\tau^{-1} = 4.9T^7 + 1.0 \times 10^7 T, \quad (8)$$

where τ^{-1} is in sec⁻¹ and T is the temperature in °K. Taking $\tau^{-1} = \frac{1}{2} \sqrt{3} \gamma W_L$ as an ansatz, Eq. (8)

leads to the dashed line plotted in Fig. 4. The extent shows the range of temperatures for which attenuation data are available. Two points are evident: (i) there is quite good agreement between these attenuation-derived linewidths and those measured by EPR, i.e., $T_2^{-1} \approx \tau^{-1}$, and (ii) over the limited "temperature window" for which both types of data are available it is difficult to discern whether Eq. (7) or Eq. (8) gives the better description. The low-temperature EPR data which favor Eq. (7) are the least accurate since they correspond to very small changes in the EPR signal. It clearly would be valuable to extend the temperature range of the ultrasonic attenuation data to resolve this question.

The approximate equality between the reorientation rate τ^{-1} and T_2^{-1} can be justified in terms of the line broadening which can occur when, due to external effects, the orientation of the distortion axis of a center jumps randomly between discrete values.¹⁵ These authors¹⁵ deal with a quadrupole split Mössbauer line and show that if $\tau^{-1} \ll 4\alpha$, the quadrupole splitting, the resonance curves have a Lorentzian shape with a width such that $T_2^{-1} = (\frac{3}{4})\tau^{-1}$. However, when $\tau^{-1} \gg 4\alpha$ the individual lines coalesce into a single Lorentzian with width $\frac{1}{3}(4\alpha)^2\tau$. In our case we therefore expect $T_2^{-1} = K\tau^{-1}$ when $\tau^{-1} \ll 2D$ where K is of order unity. Since $2D \approx 7 \times 10^{11}$ sec⁻¹ for Cr²⁺ in GaAs,¹ $\tau^{-1} \ll 2D$ is well satisfied even at 20 K. In fact, if τ^{-1} behaves like Eq. (7) with the parameters given above, one would never reach the line narrowing regime. Neither we nor VW observed a motionally narrowed spectrum for any of the tetrahedrally coordinated Cr²⁺ Jahn-Teller systems. Alternatively, one may assume that a real excited state is involved in the reorientation as the Orbach form of Eq. (7) suggests. Then the EPR linewidth will be lifetime broadened with $T_2^{-1} \approx T_1^{-1} \approx \tau^{-1}$. Lifetime broadening was previously suggested by VW. It seems clear that the EPR linewidth broadening observed by VW in the II-VI compounds also gives a measure of the reorientation rate.

The attenuation of thermally generated ballistic phonons has also been measured recently¹⁶ in GaAs:Cr at 1.5 K. The attenuation was interpreted

as due to an interaction between the phonons and those Cr centers having tetragonal symmetry (i.e., the Cr²⁺ EPR centers). In this case, however, the phonons (which have a broad frequency distribution) are thought to induce transitions between the ground-state spin energy levels of Cr²⁺. Because of the low temperature at which they were performed and their inherently poor energy resolution, these experiments were not sensitive to Cr²⁺ reorientation.

IV. SUMMARY

The stress experiments probe the static behavior of the Cr²⁺ center in GaAs and prove that the low symmetry arises from a Jahn-Teller contraction along a cube edge. They also show that the Cr²⁺ Jahn-Teller coefficient V_E is substantially larger in GaAs than in the II-VI zinc-blende compounds. In order to make the calculated splitting of the ⁵T₂ ground manifold consistent with the previously observed luminescence and optical absorption it is necessary to have a significant Jahn-Teller splitting of the excited ⁵E state with the ⁵A₁ component lowest. In agreement with the rather large E_{JT} , stress has little effect on the spin-Hamiltonian parameters.

The temperature-dependent EPR linewidths reveal the dynamics of the GaAs:Cr²⁺ center above 9 K. Comparison with recent ultrasonic attenuation results shows that this broadening is due to reorientation of the Cr²⁺ distortion axis and the linewidth parameter $T_2 \approx \tau$, the reorientation time. The experimental results indicate that τ^{-1} obeys an Arrhenius relation but can also be fit approximately by a combination of direct and T^7 Raman processes.

ACKNOWLEDGMENTS

We wish to thank E. M. Swiggard, S. H. Lee, and R. H. Bube for making crystals available to us. H. Tokomuto and V. Narayanamurti supplied us with valuable preprints of their work. Helpful discussions with M. Rubinstein on line broadening are also ack-

nnowledged. This work was supported in part by the Office of Naval Research.

APPENDIX

We consider a distributed set of Lorentzian lines $L(x)$ which are weighted according to a Gaussian envelope function $G(x)$. The resultant Voigt line shape $V(x)$ is thus

$$V(x) = \int_{-\infty}^{\infty} G(y)L(x-y) dy \quad (A1)$$

Since we normally observe the first derivative EPR signal, we actually evaluate

$$V'(x) = \int_{-\infty}^{\infty} G(y)L'(x-y) dy \quad (A2)$$

The peak-to-peak derivative widths for the Lorentzian and the Gaussian are W_L and W_G , respectively.

A computer program was written which numerically determined the Voigt peak-to-peak derivative width W_V and derivative amplitude A_V for various values of the ratio $r \equiv W_L/W_G$. It made use of 99 Lorentzian lines uniformly distributed between $\pm 1.53 W_G$. The W_V/W_G values found are in good agreement with those found previously¹⁷ and over the range $0 \leq r \leq 2$ an accurate approximation is

$$W_V = W_G(1 + 1.7r + 0.5r^2 + r^3)^{1/3} \quad (A3)$$

Over the same range we find that the following simple approximation gives a surprisingly good fit to the computer results.

$$A_V = A_G(1 + 0.783r)^{-3} \quad (A4)$$

Since normalized forms were used for $L(x)$ and $G(x)$, the integrated intensity of $V(x)$ is unity, independent of r .

For small values of r the Voigt derivative amplitude deviates from the Gaussian much more rapidly than does the linewidth. For example, at $r = 0.1$ one finds $W_V/W_G = 1.052$ but $A_G/A_V = 1.254$. Hence the EPR signal amplitude senses small r values more accurately.

¹J. J. Krebs and G. H. Stauss, Phys. Rev. B **16**, 971 (1977).

²H. Tokumoto and T. Ishiguro, J. Phys. Soc. Jpn. **46**, 84 (1979).

³J. T. Vallin and G. D. Watkins, Phys. Rev. B **9**, 2051 (1974).

⁴G. D. Watkins and J. W. Corbett, Phys. Rev. **121**, 1001 (1959).

⁵H. L. Van Camp, C. P. Sholes, and R. A. Isaacson, Rev. Sci. Instrum. **47**, 516 (1976).

⁶J. J. Krebs and G. H. Stauss, Phys. Rev. B **15**, 17 (1977).

⁷F. S. Ham, in *Electron Paramagnetic Resonance*, edited by S. Geschwind (Plenum, New York, 1972), p. 1.

⁸F. S. Ham, Phys. Rev. **166**, 307 (1968).

⁹E. J. Carlson and G. Mott, Proc. IEEE **51**, 1239 (1963).

¹⁰W. H. Koschel, S. G. Bishop, and B. D. McCombe, Solid

State Commun. **19**, 521 (1976).

¹¹J. L. T. Waugh and G. Dolling, Phys. Rev. **132**, 2410 (1963).

¹²J. T. Vallin, G. A. Slack, S. Roberts, and A. E. Hughes, Phys. Rev. B **2**, 4313 (1970).

¹³E. C. Lightowers, M. O. Henry, and C. M. Penchina, in *Physics of Semiconductors, 1978*, edited by B. L. H. Wilson, IOP Conf. No. 43 (IPPS, London, 1979), p. 307.

¹⁴D. Bois and P. Pinard, Phys. Rev. B **9**, 4171 (1974).

¹⁵J. A. Tjon and M. Blume, Phys. Rev. **165**, 456 (1968).

¹⁶V. Narayanamurti, M. A. Chin, and R. A. Logan, Appl. Phys. Lett. **33**, 481 (1978).

¹⁷H. A. Farach and H. Teitelbaum, Can. J. Phys. **45**, 2913 (1967).